Optical spectra of Si nanocrystallites: Bethe-Salpeter approach versus time-dependent density-functional theory

L. E. Ramos,[1] J. Paier,[2] G. Kresse,[2] and F. Bechstedt[1]
[1]*Institut für Festkörpertheorie und -optik, Friedrich-Schiller-Universität Jena and European Theoretical Spectroscopy Facility, Max-Wien-Platz 1, 07743 Jena, Germany*
[2]*Institut für Materialphysik, Universität Wien, Sensengasse 8/12, 1090 Wien, Austria*
(Received 3 April 2007; revised manuscript received 31 August 2008; published 21 November 2008)

Two state-of-the-art approaches based on the quasiparticle-Bethe-Salpeter equation (QP-BSE) and time-dependent density-functional theory (TDDFT) for different functionals are applied to calculate optical-absorption spectra of Si nanocrystallites passivated with hydrogen. All-electron wave functions are generated within the projector-augmented wave method. The results of the two many-body approaches are used to discuss the interplay of quasiparticle, local-field (LF), and excitonic effects. The QP approach gives rise to blueshifts of the absorption spectra, whereas the LF effects and electron-hole exchange redistribute the oscillator strengths toward higher energies. The screened electron-hole attraction leads to slightly larger optical gaps than the ones found for independent particles described within the local-density approximation (LDA) for exchange and correlation (XC). The results within the TDDFT using the LDA kernel confirm the influence of LF effects. When a hybrid functional for XC is used, the TDDFT spectra show the same tendencies as the QP-BSE ones but still indicate a reduced electron-hole attraction. An effective-medium theory is used to examine the role of local fields due to the nanocrystal arrangement.

DOI: 10.1103/PhysRevB.78.195423 PACS number(s): 73.22.−f, 71.15.Qe, 71.35.Cc, 78.67.Bf

I. INTRODUCTION

The research on Si nanocrystallites (NCs) is extremely active. Its main goal is to overcome the limitations of bulk Si as an indirect-gap semiconductor for its use in optoelectronics. There is clear experimental observation that Si nanoparticles of diameter smaller than 5 nm emit visible light[1] and even optical gain could be demonstrated.[2] The origin and the mechanism of light emission depend on the particle size, shape, passivation of dangling bonds, as well as the presence of an embedding matrix. Besides the influence of the shape and surface chemistry of the NCs, the influence of electron confinement and electron-electron interaction on the optical response is of central interest.

Silicon nanocrystallites passivated with hydrogen are suitable systems to study the light-emission intensities and frequencies from a theoretical point of view and with a variety of methods.[3–14] Since the optical properties are related to the excitation of the Si NCs, the electron-electron interaction including exchange and correlation (XC) effects has to be taken into account. Various degrees of approximations and techniques have been used such as the many-body perturbation theory (MBPT),[9–11] the time-dependent density-functional theory (TDDFT) in the adiabatic local-density approximation (LDA),[6,11,15] the delta-self-consistent-field (ΔSCF) method,[3,14] and the quantum Monte Carlo (QMC) method.[4,8,12]

The common approximation to the ground state is the LDA to the XC functional of the DFT. The eigenvalues and eigenfunctions of the Kohn-Sham (KS) equation are frequently used to calculate gaps and optical spectra within the independent-particle approximation. A comparison of energy gaps calculated with methods such as time-dependent local-density approximation (TDLDA) or ΔSCF only indicates small MBPT corrections for small Si NCs.[3,6,11,15] On the other hand, the inclusion of the electron-hole attraction within the QMC method or MBPT closes the energy gap (see Table 1 of Ref. 11), whereas the excitation effects on isolated electrons and holes open the energy gap. A tendency for cancellation of quasiparticle (QP) and electron-hole-pair effects is observed.

In contrast to the lowest pair-excitation energies, the emission and absorption spectra of Si NCs are less understood. Investigations of small Si NCs within MBPT (Refs. 9, 11, and 16) consist of a combination of QP calculations using the Hedin *GW* approximation (Green's function *G* and screened Coulomb potential *W*) for the XC self-energy[17] and the inclusion of the electron-hole interaction via a Bethe-Salpeter equation (BSE) for two-particle Green's function.[18] TDLDA investigations are performed basically within the adiabatic limit,[6,11,15,19] which can yield good results for finite systems. In particular, the bare Coulomb interaction due to local-field (LF) effects is taken into account.[20,21]

Apart from a combined TDLDA and QP-BSE study of the onset of the absorption cross section,[11] a direct comparison between the TDDFT methods with the combined treatment of the quasiparticle and electron-hole effects is still missing, in particular using the same numerical treatment and electronic structure. The reliability of the results obtained within the two approximations is still under debate. When changing from LDA to a hybrid XC function, the question that arises is how much the QP effects and electron-hole attraction can be simulated. Another open question is the influence of local-field effects (LFEs) due to the atomic structure as well as the arrangement of the nanocrystals and their consequences for spectra of isolated nanocrystals.[21,20]

In this paper we compare electronic structures and optical-absorption spectra of Si NCs with a maximum diameter of about 1.2 nm obtained within MBPT and TDDFT. After a brief description of the approximations used to deter-

mine the ground state of the NCs in Sec. II, the spectra obtained within the three different approaches, independent quasiparticles, Coulomb-correlated electron-hole pairs, and exchange-coupled electrons and holes, are presented in Secs. III–VI. The results within the schemes QP-BSE and TDDFT with two functionals are compared. Using an effective-medium theory the role of local fields is enlightened. In Sec. VII we present a summary and conclusions.

II. GROUND-STATE DESCRIPTION

As a starting point, we perform DFT calculations for the ground state with the LDA functional in the Perdew-Zunger parametrization as implemented in the Vienna *ab initio* simulation package (VASP).[22] Pseudopotentials are generated within the projector-augmented wave (PAW) method (PAW data sets),[23] which allows for all-electron wave functions suitable for the calculation of optical-transition matrix elements and matrix elements of the electron-electron interaction.[16,24] An energy cutoff of 15 Ry is applied for the plane-wave expansion of eigenfunctions. The atomic positions of the atoms in the Si NCs are determined by a shell-by-shell construction procedure, which starts from a central atom and adds shells of Si atoms successively.[14,25] This results in faceted Si NCs whose surface dangling bonds are passivated with H atoms. We allow the relaxation of the atomic positions in the Si NCs in order to minimize the interatomic forces down to less than 20 meV. Explicitly we investigate the NCs SiH_4, Si_5H_{12}, $Si_{17}H_{36}$, and $Si_{41}H_{60}$. To model the NCs, we study periodic arrangements of simple-cubic supercells with edge lengths that guarantee a distance larger than 1 nm between the surfaces of Si NCs in adjacent supercells.

III. QUASIPARTICLE GAPS

In order to include the electron-electron interaction in the excited states we use a recent implementation of the MBPT that works together with the PAW method.[16] With KS eigenvalues ε_λ and KS wave functions as starting point, we construct the self-energy operator $\Sigma(\varepsilon)$ within the *GW* approximation for XC.[17] In the computation of the frequency-dependent dielectric matrix the number of empty bands is increased until convergence is achieved, whereas in the case of the calculation of the spectra, we reduce the number of unoccupied bands in order to have only the transitions that involve states below the ionization level.[16]

The real parts of the diagonal matrix elements $\langle\lambda|\delta\Sigma(\varepsilon)|\lambda\rangle$ of the perturbation operator, $\delta\Sigma(\varepsilon)=\Sigma(\varepsilon)-V_{\mathrm{XC}}$, and the *GW* self-energy $\Sigma(\varepsilon)$ reduced by the XC potential V_{XC} already considered in the KS treatment are presented in Fig. 1. The reliability of the method, especially the neglect of the nondiagonal elements of the perturbation operator, has been described elsewhere.[16] The QP effects are stronger for excitations of occupied KS states than for those of the empty states. This is also valid for the influence of dynamical screening. For states above the Fermi level the energy variation in the self-energy is reduced since these states are less localized. The reaction of the system to a free electron is faster than the reaction to a hole in valence states. The quasiparticle energies are derived from the intersection $\varepsilon=\varepsilon_\lambda^{\mathrm{QP}}$ of $\varepsilon_\lambda+\mathrm{Re}\langle\lambda|\delta\Sigma(\varepsilon)|\lambda\rangle$ with the straight line ε in Fig. 1.

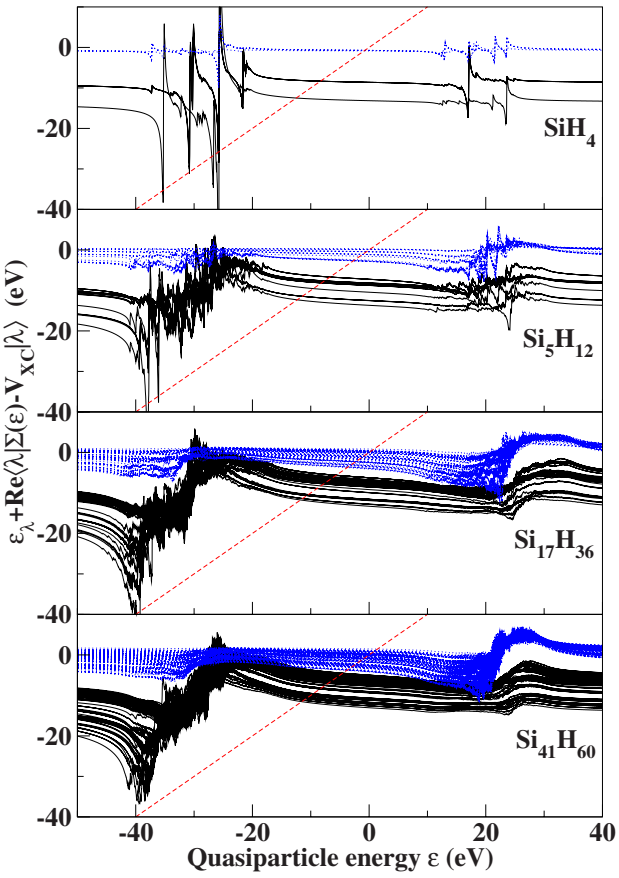

FIG. 1. (Color online) Real part of the diagonal matrix elements of the perturbation operator $\delta\Sigma(\varepsilon)$ added to the KS eigenvalues versus single-particle excitation energy. The solid (dotted) curves represent filled (empty) states. The straight dashed line is $f(\varepsilon)=\varepsilon$.

For an approximate description of the single-particle excitation energies within the TDDFT beyond the adiabatic local-density approximation (TDLDA), we apply a hybrid functional for XC according to Heyd, Scuseria, and Ernzerhof (HSE) (Ref. 26) to derive an XC potential in the generalized Kohn-Sham (GKS) equation or in a quasiparticle equation where the XC self-energy is approximated by the density variation in the HSE-XC functional.[27] In the following we refer to this TDDFT approach as time-dependent Heyd-Scuseria-Ernzerhof (TDHSE). It has been shown that the eigenvalues $\varepsilon_\lambda^{\mathrm{GKS}}$ and associated wave functions are an excellent starting point to solve the quasiparticle problem self-consistently for both semiconductors and insulators.[28] The HSE functional combines 25% of the bare nonlocal exchange and 75% of a screened nonlocal exchange with an explicit local-density functional.[26]

The differences between the highest occupied molecular-orbital (HOMO) and the lowest unoccupied molecular-orbital (LUMO) states, i.e., the independent-(quasi)particle gap as well as the lowest pair energy E_{pair} with electron-hole interaction, the optical gap, are presented in Table I. For all approaches, Table I exhibits a clear trend for decreasing qua-

TABLE I. The lowest pair-excitation energies (in eV) E_{pair} of Si NCs: quasiparticle gaps within KS approach with LDA functional, GKS with nonlocal HSE functional, or QP within *GW* approximation; optical gaps within TDLDA, TDHSE, or QP-BSE and corresponding approximations with vanishing XC kernel ($K_{\text{XC}}=0$ or vanishing electron-hole attraction $W=0$). For comparison the excitation energies from other calculations are given in parentheses: KS (Ref. 11), TDLDA (Refs. 6 and 11), and QP-BSE (Ref. 9).

	Quasiparticle gap			Optical gap					
Nanocrystallite	KS	GKS	QP	TDLDA	TDHSE	QP-BSE	TDLDA ($K_{\text{XC}}=0$)	TDHSE ($K_{\text{XC}}=0$)	QP-BSE ($W=0$)
SiH_4	7.95 (7.9)	8.80	12.72	8.01 (8.2, 8.2)	8.65	8.29 (9.0)	8.09	8.92	12.94
Si_5H_{12}	5.64 (5.7)	6.60	10.83	5.68 (6.6, 5.8)	6.31	6.86 (6.6)	5.69	6.63	10.18
$Si_{17}H_{36}$	4.20 (4.1)	5.03	8.09	4.28 (4.3)	4.94	5.90	4.32	5.18	8.23
$Si_{41}H_{60}$	3.25	3.96	6.19	3.27	3.88	4.63	3.29	4.02	6.24

siparticle gaps with increasing diameter of the Si NCs. For the KS approach and TDLDA our values of the lowest pair energies agree with previous results.[11] The deviations of the order of 0.1 eV indicate the influence of numerical details such as pseudopotentials, wave functions, and relaxed geometries.

The advantages of using the hybrid HSE functional over the LDA functional can be seen from the gap values of Table I and in the spectra of Fig. 2. In the limit of vanishing Coulomb correlation of electrons and holes, the GKS-HSE fundamental gaps are blueshifted by 0.7–0.9 eV with respect to the KS-LDA ones. However, the large blueshifts of 2.9–5.2 eV due to the QP effects are not reached since the HSE functional does not describe correctly single-(quasi)particle excitations in finite systems.

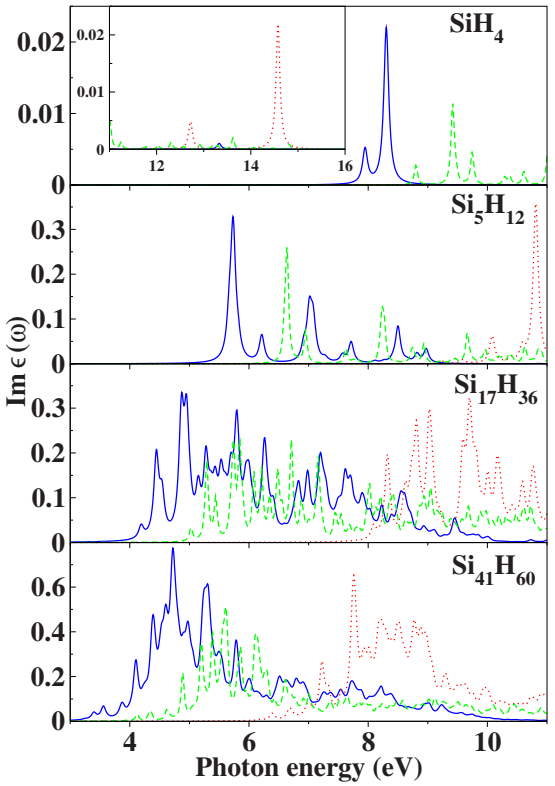

FIG. 2. (Color online) Imaginary part of the dielectric function versus energy in independent-particle or quasiparticle approximation: KS-LDA (blue solid line), GKS-HSE (green dashed line), and QP-*GW* (red dotted line). The insets show the spectrum at high energies.

IV. ELECTRON-HOLE PAIR EXCITATIONS

The solution of the BSE for the polarization function yields the optical-absorption spectrum. We use an initial-state formulation in which the time evolution is described by a two-particle Hamiltonian.[24] Neglecting the coupling between resonant and antiresonant contributions to the polarization and restricting to spin-singlet pairs, we apply a two-particle Hamiltonian combining interacting quasielectrons in states $\lambda=e$ and quasiholes in single-particle states $\lambda=h$ of the form

$$H(eh,e'h') = [\varepsilon_e^{\text{QP}} - \varepsilon_h^{\text{QP}}]\delta_{ee'}\delta_{hh'} - W(eh,e'h') + 2\bar{v}(ee',hh') \tag{1}$$

with the statically screened Coulomb attraction

$$W(eh,e'h') = \int d^3\mathbf{x} \int d^3\mathbf{x}'\, \psi_e^*(\mathbf{x})\psi_{e'}(\mathbf{x})W(\mathbf{x},\mathbf{x}';0)\psi_h(\mathbf{x}')\psi_{h'}^*(\mathbf{x}') \tag{2}$$

between electrons and holes, which couples two pairs eh and $e'h'$ characterized by the KS wave functions $\psi_e(\mathbf{x})$ and $\psi_h(\mathbf{x})$. In the screened Coulomb potential $W(\mathbf{x},\mathbf{x}';\omega=0)$ the screening is described by the inverse dielectric matrix computed in the QP approach (Sec. III). Because only singlet pair states are of interest for the optical properties, the unscreened electron-hole exchange interaction,

$$\bar{v}(ee',hh') = \int d^3\mathbf{x} \int d^3\mathbf{x}'\, \psi_e^*(\mathbf{x})\psi_h(\mathbf{x})\bar{v}(\mathbf{x}-\mathbf{x}')\psi_{e'}(\mathbf{x}')\psi_{h'}^*(\mathbf{x}'), \tag{3}$$

with the short-range contribution $\bar{v}(\mathbf{x}-\mathbf{x}')$ of the bare Coulomb potential is multiplied by 2 in Eq. (1).[24] This term couples two quasielectron-quasihole pairs as well. For crystalline bulk systems it was shown that this interaction can be identified with LF effects.[29,30]

The values of the lowest energy eigenvalues of exciton Hamiltonian (1) are listed in Table I. The QP-BSE pair en-

ergies vary almost linearly versus the reciprocal NC diameter. A comparison between E_{pair}(QP) and E_{pair}(QP-BSE) shows the effect of the effective electron-hole attraction. The difference between QP gap and the lowest energy E_{pair}(QP-BSE) of two-particle Hamiltonian (1) gives the effective binding energies of the lowest electron-hole pairs between 4.4 eV (SiH_4) and 1.6 eV ($Si_{41}H_{60}$). The effective binding energies significantly decrease from the molecular structures SiH_4 and Si_5H_{12} to the intermediate-size NCs $Si_{17}H_{36}$ and $Si_{41}H_{60}$. Our values of binding energies agree with the 3.9–2.4 eV predicted in Ref. 11 or 3.7 eV (SiH_4) in Ref. 9 but exhibit a stronger size dependence, which is almost linear with the reciprocal NC radius. The deviations may be interpreted as consequences of the use of a model dielectric function[11] or a Gaussian-orbital represented of the single-particle wave functions.[9] The lowest excitonic excitation energies in Table I for the two smallest clusters are in almost agreement with experimental values of 8.8 eV (silane)[31] and 6.5 eV (pentasilane).[32] The dominating electron-hole interaction in Eq. (1) is the screened Coulomb attraction. The comparison of QP and QP-BSE ($W=0$) values in Table I indicates a reduced influence of LF and electron-hole exchange effects on the absorption onsets. With exception of Si_5H_{12} the electron-hole exchange tends to an extremely small blueshift of the lowest pair energy of about 0.1 eV with a tendency to vanish for large NCs. The QP-BSE pair energies are only slightly larger than the KS energies E_{pair}(KS) in Table I. This fact indicates an almost compensation of QP blueshifts and redshifts due to electron-hole attraction as discussed previously.[3,6,11,12] However, the compensation effect decreases with rising diameter toward the dominance of QP shifts in the bulk limit.[24]

In order to describe the role of the electron-electron interaction in the optical-absorption spectra within the TDDFT, two of the authors have implemented the formulation of the density response by Stratmann *et al.*[33] in VASP.[34] The linear response of the density matrix is given by an operator similar to electron-hole-pair Hamiltonian (1). The resonant part is

$$\tilde{H}(eh,e'h') = [\varepsilon_e^{\mathrm{GKS}} - \varepsilon_h^{\mathrm{GKS}}]\delta_{ee'}\delta_{hh'} + K(eh,e'h'), \quad (4)$$

where the coupling matrix

$$K(eh,e'h') = K_{\mathrm{XC}}(eh,e'h') + 2v(ee',hh') \quad (5)$$

is given by the matrix elements of the second variation in the DFT XC functional with respect to the density, $K_{\mathrm{XC}} = \delta^2 E_{\mathrm{XC}}/\delta n(\mathbf{x})\delta n(\mathbf{x}')$. K_{XC} replaces the screened electron-hole attraction $W(\mathbf{x},\mathbf{x}';0)$ in the matrix element in Eq. (2). In the TDDFT the wave functions are replaced by the GKS ones and treated in the adiabatic approximation, i.e., independent of time or frequency. After the correct treatment of the electron and hole spins for singlets, the second term v in Eq. (5) corresponds to electron-hole exchange effects, although it is not restricted to the short-range part. In contrast to QP-BSE treatment (1), within the TDDFT we also take into account the coupling matrix $K(eh,h'e')$ in Eq. (5) between resonant and antiresonant transition terms. Despite the formal similarities between Eqs. (1) and (4) with respect to the electron-hole interaction, we notice that the independent-particle or quasiparticle contribution with $K=0$ is different. In the TDDFT the eigenvalues $\varepsilon_\lambda^{\mathrm{GKS}}$ of the KS or GKS approach are used, whereas the QP-BSE approach uses the true single-particle excitation energies $\varepsilon_\lambda^{\mathrm{QP}}$. We study two XC functionals E_{XC}, which are the LDA (TDLDA) and the hybrid HSE functional (TDHSE).[26]

In the case of the lowest pair-excitation energies (Table I) the TDLDA and TDHSE yield similar values as the KS or GKS approaches. The corresponding gaps are only slightly smaller in the TDHSE case compared to GKS by about 0.1 eV. The absolute TDLDA values are comparable with those from other calculations.[6,11] The average deviation amounts to 0.1 eV or less. The overestimation in the Si_5H_{12} case with 6.6 eV is probably a consequence of the underlying KS description.[6] The TDHSE energies are significantly increased by 0.5–0.6 eV with respect to the TDLDA results. However, the differences are smaller than those between the KS and GKS gaps. The latter values are widely recovered in the limit of $K_{\mathrm{XC}} \equiv 0$ confirming the small effect of the electron-hole exchange on the absorption onset. The increase in the optical gaps from TDLDA to TDHSE is mainly a consequence of the blueshift due to the replacement of the KS eigenvalues by the GKS ones. The differences between the quasiparticle gaps in GKS and the optical gaps from TDHSE are rather small and hence indicate that the Coulomb effects described by kernel (5) do hardly influence the value of the lowest pair energy as already found for the QP-BSE approach. Both quasiparticle and excitonic effects are reduced for the absorption onset in TDHSE compared to QP-BSE, at least for the larger clusters Si_5H_{12}, $Si_{17}H_{36}$, and $Si_{41}H_{60}$, by about 0.5–1.0 eV.

V. OPTICAL ABSORPTION SPECTRA

The frequency-dependent imaginary parts of the macroscopic dielectric function $\epsilon(\omega)$ of Si NC arrangements are shown in Figs. 2–4 for nine approximations of the XC part of the electron-electron interaction. A Lorentzian broadening of 0.05 eV is used in all spectra. The TDLDA and TDHSE take into account an equal number of conduction bands as in the QP screening. In Fig. 2 as the NC size increases, the absorption onsets gradually decrease, and the discrete spectra of small clusters evolve into quasicontinuous spectra. At the same time, the oscillator strength of the dipole-allowed optical transitions near the absorption edge decreases with increasing cluster size. This trend for Si NCs is consistent with an indirect band gap of bulk Si.[6,14,25] The inclusion of the quasiparticle shifts of the electron and hole levels within the approximation of independent quasiparticles does practically not change the line shape of the spectra in Fig. 2. Except for SiH_4 and Si_5H_{12}, the inclusion of QP shifts leads to an overall blueshift similar to the case of bulk Si.[24] The spectra of independent GKS particles exhibit similar line shapes, not only with the HSE functional but also within LDA, at least for large NCs. However, the blueshift is much smaller than in the QP case, as discussed above for the energy gaps in Table I.

The effects of the Coulomb interaction of quasielectrons and quasiholes in Fig. 3 act in a completely different way compared with bulk Si. In the QP-BSE approach the

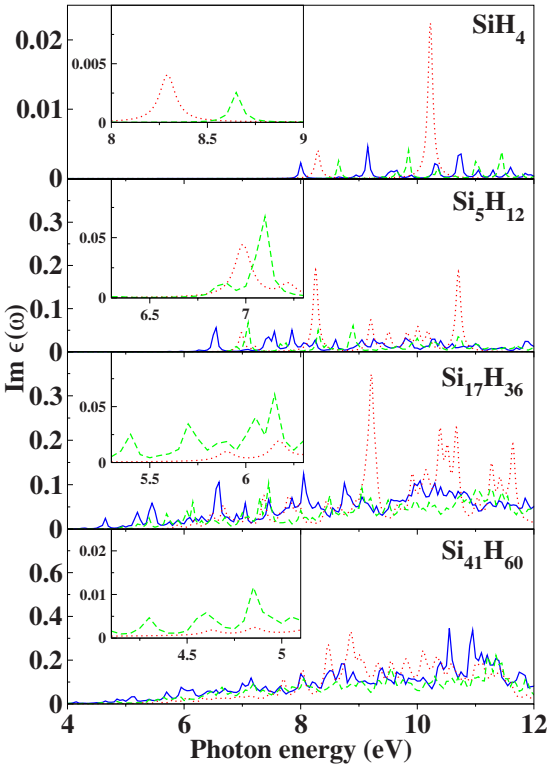

FIG. 3. (Color online) Imaginary part of the dielectric function versus energy in time-dependent density-functional theory or exciton description: TDLDA (blue solid line), TDHSE (green dashed line), and QP-BSE (red dotted line). The insets show the spectrum near the onset of absorption.

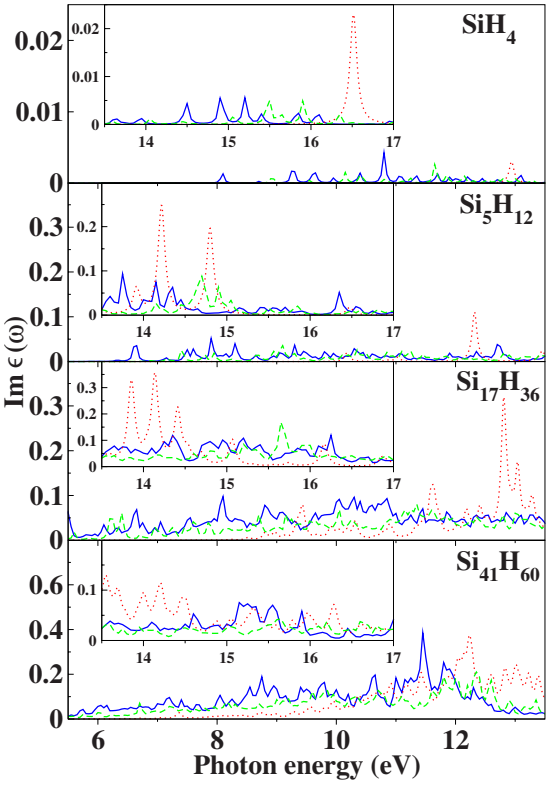

FIG. 4. (Color online) Imaginary part of the dielectric function versus energy in same approximation as in Fig. 3 but restricting the Coulomb correlation of electron-hole pairs to the electron-hole exchange or LF effects: TDLDA with $K_{XC}=0$ (blue solid line), TDHSE with $K_{XC}=0$ (green dashed line), and QP-BSE with $W=0$ (red dotted line). The insets show the spectra at high energies.

electron-hole attraction effects lead to a redshift of the bulk absorption spectrum associated with a redistribution of oscillator and spectral strengths from higher energies to low photon energies.[24] For the smallest Si clusters, similar excitonic effects are visible, whereas for clusters of intermediate size such as $Si_{17}H_{36}$ or $Si_{41}H_{60}$, the excitonic effects including exchange yield a remarkable redistribution of oscillator strength over a wide range of photon energies accompanied by a reduction in the maximum spectral strengths compared to the QP-*GW* spectrum in Fig. 2. There are also optical transitions below the absorption edge E_{pair} (QP) of the uncorrelated quasielectron-quasihole pairs indicating bound exciton states. However, the most important effect remains the spectral distribution over a much wider energy range, which we only show until 12 eV. We also observe an enhancement of the oscillator strength of high-energy excitations, leaving less strength in the central regions of the absorption spectra. Qualitatively a similar many-body influence is observed in the TDLDA and TDHSE spectra in comparison with the results obtained within the independent-particle approximation. For the small clusters SiH_4 and Si_5H_{12}, TDLDA and TDHSE tend to blueshift (redshift) the spectra with respect to the independent-particle limit. For large clusters, which are still much smaller than the wavelength of light, the spectra shift to high photon energies compared to Fig. 2 (see also energy gaps in Table I).

Despite the reasonable agreement for the absorption edges within the three approximations used and the trends with respect to the spectral distributions, we find different spectra in Fig. 3 within the three approximations, QP-BSE, TDLDA, and TDHSE. This holds especially for the line shape at high frequencies where the QP-BSE gives rise to higher peak intensities. However, from Table I and the onsets in Fig. 3 we also see differences at the absorption edges. Both QP shifts and electron-hole attraction are underestimated within the TDDFT approaches. In contrast to the lowest pair energies, for Si NCs in this scheme we cannot confirm the statements that suggest TDLDA is good for confined systems.[11,21] Rather, we agree with Tiago and Chelikowsky[7] that TDLDA and QP-BSE are significantly different. Only for intermediate-size clusters, here $Si_{41}H_{60}$, the deviations are much smaller. Within the TDDFT approaches the effect of K_{XC} [Eq. (5)] seems to be negligible in comparison with the QP effects. K_{XC} and QP effects do not compensate each other in the spectra. The improvement of the approximation for the XC kernel within the TDHSE mostly brings the spectra closer to the QP-BSE ones. There is indeed a blueshift of the transition energies from LDA to HSE. Also electron-hole attraction occurs in TDHSE. The inclusion of 25% of Fock exchange may be interpreted to result in a screened electron-hole attraction in Eq. (5) with a screening dielectric constant, whose value of about 4 is much larger than the values of 1.1–1.4 predicted for Si clusters.[12] The Coulomb attraction is hence much weaker in TDHSE than in QP-BSE. However,

we have to mention that we do not consider the effect of the resonant-antiresonant coupling in QP-BSE, which was taken into account within the TDDFT. However, for the smallest cluster SiH_4 it has been shown that this coupling only gives rise to a small redshift.[35]

VI. LOCAL-FIELD EFFECTS

There are discussions in the literature claiming that the tendency for redistribution of spectral strength over a wide range of photon energies in the imaginary part of the dielectric function within QP-BSE is mostly a consequence of the repulsive electron-hole exchange or the LF effects due to $2\bar{v}$ in Eq. (1).[11,36] Such a redistribution is seemingly enhanced due to the spatial confinement of the wave functions as shown in Fig. 3. The electron-hole exchange is also present in TDLDA and TDHSE in the form of the bare Coulomb potential $2v$ in the integral equation for the response function in Eq. (5) (Ref. 11) and can be identified with LF effects as $2\bar{v}$ in Eq. (1).[36] In order to understand the role of the electron-hole exchange effects and, hence, the LFE in the case of Si NCs of intermediate size we neglect the direct screened Coulomb attraction $-W$ and study the pure effect of $2\bar{v}$ in Eq. (1) or $2v$ in Eq. (5). Corresponding results are presented in Fig. 4. They make visible that although TDLDA and TDHSE fail to predict correctly the influence of the electron-hole attraction on the optical absorption of Si NCs,[7] they give rise to similar tendencies—mainly spectral distribution over a wider energy range—due to electron-hole exchange or LF effects. Thereby, they happen for different (quasi)particle energy differences. Nevertheless, the spectra are significantly changed compared with the quasiparticle ones in Fig. 2. In Fig. 4 much more intensity occurs at higher energies as visible in the insets.

In order to understand the role of the bare Coulomb interaction for confined systems, from a more qualitative point of view, we follow the discussion by Sottile *et al.*[21] In the language of TDDFT the approximation $K_{XC}=0$ in Eq. (5) is called random-phase approximation (RPA). It leads formally to a susceptibility $\chi(\omega)=\chi_0(\omega)/[1-v\chi_0(\omega)]$ with $\chi_0(\omega)$ being the susceptibility of the independent KS or GKS particles. With respect to the complete TDLDA, TDHSE, and QP-BSE results in Fig. 3, the neglect of K_{XC} or $-W$ leads to large (QP-BSE) or small (TDLDA and TDHSE) blueshifts of the spectra and to a redistribution of the spectral strength toward high photon energies in Fig. 4. This is mainly a consequence of the plasmonic denominator $[1-v\chi_0(\omega)]$ in the frequency-dependent polarization. The inclusion of K_{XC} or $-W$ in the spectra as shown in Fig. 3 tends to overcome the exchange or LF effects and to redistribute the spectral strength toward small photon energies. The contributions of the electron-hole attraction and the electron-hole exchange are more important within the MBPT scheme. The absence of $-W$ (Fig. 4) leads to a blueshift of the QP-BSE spectra much more pronounced than within the TDLDA and TDHSE. In contrast to the bulk situation, for the clusters under consideration the electron and hole wave functions are strongly localized and their considerable overlap yields non-negligible v matrix elements.

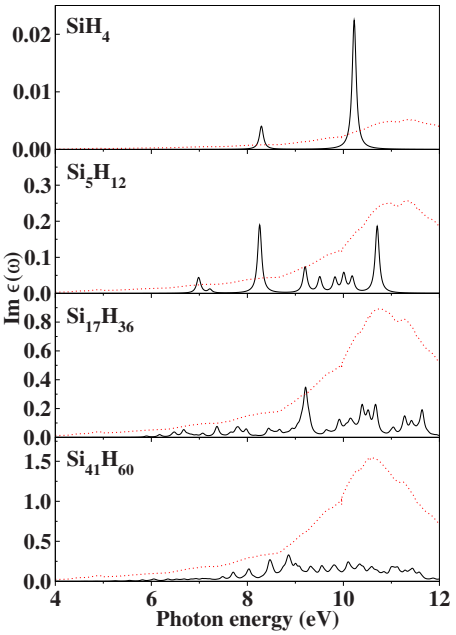

FIG. 5. (Color online) Imaginary part of the dielectric function from the Maxwell Garnett EMT (6) (Ref. 37) using Si bulk dielectric function for NCs (red dotted line). It is compared with the function (black solid line) obtained within the QP-BSE scheme for the confined system (cf. Fig. 3).

The spectra represented in Figs. 2–4 correspond to a three-dimensional arrangement of Si NCs in unit cells of a simple-cubic lattice. Each unit cell contains one NC surrounded by vacuum. In addition to LF effects due to the atomic structure of the NCs, there are also those related to the spatial arrangement of the NCs.[20] The role of those local-field effects related to NC neighbors can be investigated in the framework of an effective-medium theory (EMT), e.g., the Maxwell Garnett one.[37] In this description the dielectric function $\epsilon(\omega)$ computed for the NCs in the supercell arrangement is related to that of an isolated NC (quantum dot) $\epsilon_{NC}(\omega)$. For the imaginary part it holds

$$\mathrm{Im}\ \epsilon(\omega) = -\frac{9f}{(1-f)^2}\mathrm{Im}\frac{1}{\epsilon_{NC}(\omega)+\dfrac{2+f}{1-f}}, \tag{6}$$

$$\mathrm{Im}\ \epsilon_{NC}(\omega) = -\frac{9f}{(1-f)^2}\mathrm{Im}\frac{1}{\epsilon(\omega)-\dfrac{1+2f}{1-f}}, \tag{7}$$

where f is the effective filling factor of the NC arrangement describe above. For a first test in Fig. 5 we have neglected the confinement effects in $\epsilon_{NC}(\omega)$ and replaced $\epsilon_{NC}(\omega)$ by $\epsilon_{Si}(\omega)$, the dielectric function of Si bulk. We use a function calculated within the QP-BSE approach including QP, excitonic, and atomic LF effects.[24] In Fig. 5 results from Eq. (6) are compared with QP-BSE NC spectra from Fig. 3 where all Coulomb interactions between electrons and holes are included. Figure 5 makes more visible the above-discussed trend. The three-dimensional arrangement of the Si NCs

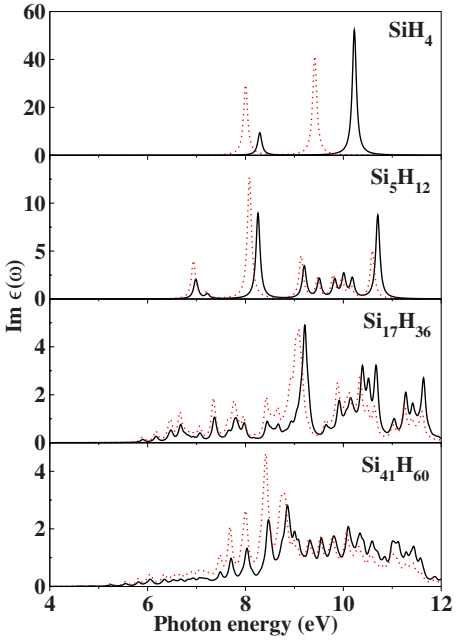

FIG. 6. (Color online) Absorption spectra for isolated nanocrystallites Im $\epsilon_{NC}(\omega)$ from Maxwell Garnett formula (7) (Ref. 37) using QP-BSE dielectric functions from Fig. 3. For the purpose of comparison the spectra from Fig. 3 divided by the fraction f are plotted as solid black lines.

leads to a spectrum that is significantly modified compared to the spectrum of an isolated NC, here represented by that of bulk Si. The tendency of redistribution to higher photon energies is clearly a consequence of the effective medium described by formula (6). The high-spectral strength at photon energies in the region of 10–12 eV describes more surface-like plasmon features than electron-hole pair excitations in the isolated cluster. Both the line shape and the spectral strength depend of course remarkably on the filling factor of the NC arrangement. For $f \rightarrow 1$ the NC absorption becomes visible while for smaller filling factors the plasmonic character dominates. Figure 5 clearly shows that LFE due to the NC arrangement dramatically modifies the silicon nanocrystal optical response at variance with bulk silicon. One of the most important influences is the surface electronic polarization which is already included in a classical dielectric model.[20] However, Fig. 5 also demonstrates that for extremely small Si NCs with diameters down to about 1 nm or less the quantum confinement effects have to be taken into account and that an EMT can only describe the correct trends.

The physics included in the Maxwell Garnett EMT (Ref. 37) also allows us to extract the dielectric function of an isolated nanocrystal $\epsilon_{NC}(\omega)$ from the dielectric function $\epsilon(\omega)$ of the supercell arrangement computed for the Si NC arrangement and including electronic confinement and many-body (quasiparticle, electron-hole attraction, and electron-hole exchange) interactions. Using formula (7) and the QP-BSE spectra $\epsilon(\omega)$ from Fig. 3 the results are plotted in Fig. 6 for the imaginary parts, i.e., basically (apart from a factor $\sim\omega$) the absorption spectra. In addition, the spectra are shown for an effective dielectric function $\epsilon_{eff}(\omega)$ with $\epsilon(\omega) = f\epsilon_{eff}(\omega) + (1-f)$, which are enhanced by $1/f$ in comparison to those in Fig. 3. The absorption spectra of the isolated NCs are significantly changed with respect to those of the supercell arrangement in Fig. 3. This holds for both the magnitude and the line shape. One observes two important features. (i) The spectrum obtained for the supercell arrangement is slightly redistributed to lower photon energies. For large filling factors $f \rightarrow 1$ this is a consequence of the negative sign of the term $(1+2f)/(1-f)$ in formula (7). The poles in $\epsilon^{-1}(\omega)$ are shifted to lower energies. (ii) Due to the concentration on the NCs and hence smaller volumes per cluster the intensities are enhanced (at least for the smallest one) toward the maximum values of Im $\epsilon_{NC}(\omega) \sim 50$ observed in bulk silicon. Similar tendencies have been found in experimental studies.[38–40] Arrangements of Si nanocrystals in a SiO_2 matrix have been studied by means of spectroscopic ellipsometry. The resulting spectra have been traced back to those of isolated NCs using an effective-medium approximation, Maxwell Garnett[37,38,40] or Bruggeman[39] one. However, the spectra in Fig. 6 are less redistributed toward lower photon energies, at least not into the region of the bulk E_1 and E_2 transitions. Moreover, still a huge number of peaks are visible. One possible reason for the discrepancies may be the influence of the amorphous SiO_2 matrix in the experimental spectra, which in any case gives rise to a drastic reduction in the optical-transition energies of the SiNCs.[14]

VII. SUMMARY AND CONCLUSIONS

In summary, we have calculated the optical-absorption spectra of Si NCs passivated with H within the MBPT and TDDFT. Within the first method the (dynamical) screening reaction of the electronic system to the excitation of interacting electrons and holes has been fully calculated based on the *GW* approximation for the self-energy and the homogeneous BSE. We have shown that, in contrast to bulk Si, both the screened electron-hole attraction and the unscreened electron-hole exchange have to be taken into account to describe the absorption spectra of NCs. The repulsive exchange interaction, which corresponds to local-field effects, is responsible for a wide spectral distribution toward high photon energies. On the other hand, the electron-hole attraction is important to obtain correct energy positions of the spectral features. Especially the absorption onsets are dominated by the screened electron-hole attraction. The accompanying redshifts are however almost compensated by the gap widenings due to quasiparticle effects.

The TDDFT approximation supports the central role of electron-hole exchange or local-field effects for the line shape of absorption spectra of intermediate sizes of Si NCs. This is true for the spectral distributions and for the peak positions. Within TDDFT the absorption onsets are less influenced by the electron-hole interaction. The qualitative similarities between the TDLDA, TDHSE, and QP-BSE results for the absorption edge are a consequence of the tendency for cancellation of the nonlocal XC effects and the electron-hole attraction, which increase and decrease the transition energies, respectively. The treatment of both effects in three different approximations gives rise to under-

standable differences. The relatively weak variation in the position of the absorption edge for a given confined system does not allow the conclusion that TDDFT with an adiabatic treatment of local (LDA) or nonlocal (HSE) XC kernels gives rise to optical spectra in agreement with the results of the full inclusion of the electron-hole interaction within the QP-BSE scheme. The reason is that the almost cancellation of the quasiparticle and excitonic effects close to the absorption edge is not anymore fulfilled at higher photon energies. As a consequence the line shapes (in Fig. 3) remain different in spite of similar tendencies observable in the three considered approximations QP-BSE, TDLDA, and TDHSE. Within the TDDFT approaches the electron-hole attraction is almost missing or at least significantly suppressed. Consequently, for a reliable description of the optical properties of nanocrystallites we suggest the use of the QP-BSE scheme not only for the large bulklike nanocrystallites but also for those of intermediate size. Even for the molecules differences in the line shape between QP-BSE and TDLDA schemes are visible. The only way to improve the TDDFT scheme is the improvement of the kernels to describe better the effect of the screened Coulomb interaction and, hence, vertex corrections.

The local-field effects play an important role for the line shape of the absorption spectra of the various NC arrangements studied for different NC diameters and filling factors. They are partially included in the three approximations used for the spectra calculations on a similar level. They tend to a distribution of spectral strengths toward higher photon energies as a consequence of plasmonic effects. This has been clearly demonstrated using an effective-medium theory. Not only the confinement effects and the electron-electron interaction in an isolated nanocrystallite but also the three-dimensional arrangement of the clusters influence the line shape of the optical absorption. The opposite tendency has been observed by extracting the dielectric function of isolated Si nanocrystals from the spectra calculated within the QP-BSE approach for three-dimensional arrangements of the nanocrystallites.

ACKNOWLEDGMENTS

This work was supported by the Austrian FWF (SFB25 IR-ON), the European Community in the framework of the Network of Excellence NANOQUANTA (Contract No. NMP4-CT-2004-500198), and the Federal Ministry of Education and Research of Germany (Project No. 03SF0308). A grant of computer time from NIC Jülich (Project No. HJN21, 2006) is gratefully acknowledged.

[1] M. V. Wolkin, J. Jorne, P. M. Fauchet, G. Allan, and C. Delerue, Phys. Rev. Lett. **82**, 197 (1999).
[2] L. Pavesi, L. D. Negro, C. Mazzoleni, G. Franzò, and F. Priolo, Nature (London) **408**, 440 (2000).
[3] H.-Ch. Weissker, J. Furthmüller, and F. Bechstedt, Phys. Rev. B **67**, 245304 (2003); **69**, 115310 (2004).
[4] J. C. Grossman, M. Rohlfing, L. Mitas, S. G. Louie, and M. L. Cohen, Phys. Rev. Lett. **86**, 472 (2001).
[5] R. Del Sole, G. Adragna, V. Olevano, and L. Reining, Phys. Rev. B **67**, 045207 (2003).
[6] I. Vasiliev, S. Öğüt, and J. R. Chelikowsky, Phys. Rev. Lett. **86**, 1813 (2001).
[7] M. L. Tiago and J. R. Chelikowsky, Phys. Rev. B **73**, 205334 (2006).
[8] E. W. Draeger, J. C. Grossman, A. J. Williamson, and G. Galli, Phys. Status Solidi B **239**, 11 (2003).
[9] M. Rohlfing and S. G. Louie, Phys. Rev. Lett. **80**, 3320 (1998).
[10] C. Delerue, G. Allan, and M. Lannoo, Phys. Rev. Lett. **90**, 076803 (2003).
[11] L. X. Benedict, A. Puzder, A. J. Williamson, J. C. Grossman, G. Galli, J. E. Klepeis, J.-Y. Raty, and O. Pankratov, Phys. Rev. B **68**, 085310 (2003).
[12] S. Öğüt, R. Burdick, Y. Saad, and J. R. Chelikowsky, Phys. Rev. Lett. **90**, 127401 (2003).
[13] A. Puzder, A. J. Williamson, J. C. Grossman, and G. Galli, J. Am. Chem. Soc. **125**, 2786 (2003).
[14] L. E. Ramos, J. Furthmüller, and F. Bechstedt, Phys. Rev. B **70**, 033311 (2004); Appl. Phys. Lett. **87**, 143113 (2005).
[15] A. Tsolakidis and R. M. Martin, Phys. Rev. B **71**, 125319 (2005).
[16] P. H. Hahn, W. G. Schmidt, and F. Bechstedt, Phys. Rev. B **72**, 245425 (2005).
[17] L. Hedin, Phys. Rev. **139**, A796 (1965).
[18] L. J. Sham and T. M. Rice, Phys. Rev. **144**, 708 (1966).
[19] I. Vasiliev and R. M. Martin, Phys. Rev. A **69**, 052508 (2004).
[20] F. Trani, D. Ninno, and G. Iadonisi, Phys. Rev. B **75**, 033312 (2007).
[21] F. Sottile, F. Bruneval, A. G. Marinopoulos, L. K. Dash, S. Botti, V. Olevano, N. Vast, A. Rubio, and L. Reining, Int. J. Quantum Chem. **102**, 684 (2005).
[22] G. Kresse and J. Furthmüller, Phys. Rev. B **54**, 11169 (1996); Comput. Mater. Sci. **6**, 15 (1996).
[23] G. Kresse and D. Joubert, Phys. Rev. B **59**, 1758 (1999).
[24] W. G. Schmidt, S. Glutsch, P. H. Hahn, and F. Bechstedt, Phys. Rev. B **67**, 085307 (2003).
[25] L. E. Ramos, J. Furthmüller, and F. Bechstedt, Phys. Rev. B **72**, 045351 (2005).
[26] J. Heyd, G. E. Scuseria, and M. Ernzerhof, J. Chem. Phys. **118**, 8207 (2003).
[27] A. Seidl, A. Görling, P. Vogl, J. A. Majewski, and M. Levy, Phys. Rev. B **53**, 3764 (1996).
[28] F. Fuchs, J. Furthmüller, F. Bechstedt, M. Shishkin, and G. Kresse, Phys. Rev. B **76**, 115109 (2007).
[29] W. Hanke and L. J. Sham, Phys. Rev. Lett. **43**, 387 (1979).
[30] R. Del Sole and E. Fiorino, Phys. Rev. B **29**, 4631 (1984).
[31] U. Itoh, Y. Toyoshima, H. Onuki, N. Washida, and T. Ibuki, J. Chem. Phys. **85**, 4867 (1986).
[32] B. Delley and E. F. Steigmeier, Phys. Rev. B **47**, 1397 (1993).
[33] R. E. Stratmann, G. E. Scuseria, and M. J. Frisch, J. Chem. Phys. **109**, 8218 (1998).

[34] J. Paier, M. Marsman, K. Hummer, G. Kresse, I. C. Gerber, and J. G. Ángyán, J. Chem. Phys. **124**, 154709 (2006).
[35] F. Bechstedt, C. Rödl, L. E. Ramos, F. Fuchs, P. H. Hahn, and J. Furthmüller, Proceedings of the Ninth EPIOPTICS School, Erice 2006 (World Scientific, Singapore, 2007).
[36] M. Gatti and G. Onida, Phys. Rev. B **72**, 045442 (2005).
[37] J. C. Maxwell Garnett, Philos. Trans. R. Soc. London, Ser. A **203**, 385 (1904).
[38] L. Ding, T. P. Chen, Y. Liu, C. Y. Ng, and S. Fung, Phys. Rev. B **72**, 125419 (2005).
[39] B. Gallas, I. Stenger, C.-C. Kao, S. Fisson, G. Vuye, and J. Rivory, Phys. Rev. B **72**, 155319 (2005).
[40] L. Ding, T. P. Chen, Y. Liu, M. Yang, J. I. Wong, Y. C. Liu, A. D. Trigg, F. R. Zhu, M. C. Tan, and S. Fung, J. Appl. Phys. **101**, 103525 (2007).